Comparison of Concurrent Radar and Aircraft Measurements of Cirrus Clouds

Nicholas Gapp
M.S. Thesis Defense
University of North Dakota
Grand Forks, North Dakota
2019/06/07

Committee Members:
Dr. David Delene*, UND
Dr. Matthew Gilmore, UND
Dr. Jerome Schmidt, NRL-MRY
Dr. Paul Harasti, NRL-MRY

* Committee Chair

Motivation for Research

- Cirrus clouds are important
  - Everywhere
  - Tough to model and predict
  - More understanding is needed to derive vertically integrated cloud water content
- Many previous studies and field projects have researched cirrus clouds
  - Cirrus Regional Study of Tropical Anvils and Cirrus Layers—Florida Area Cirrus Experiment (CRYSTAL-FACE) (Jensen et al. 2004)

CRYSTAL-FACE

- Summer 2002 field project in southern Florida
- Studied cirrus cloud shields from deep convection
  - Six aircraft including North Dakota Cessna Citation II Research Aircraft
- A couple goals:
  - Study physical processes in and properties of cirrus anvils
  - Dependence of cirrus properties on strength of convection and state of environment
- Found that anvil ice crystals are smaller and more reflective than what was assumed in global climate models of the day
  - Among many other findings

The CAPE2015 Field Experiment

- Near Cape Canaveral, Florida, from 28 July to 11 August, 2015
- Studied cirrus cloud anvils from Florida thunderstorms
- Different from other studies
  - Concurrent measurements between in-situ (aircraft) and remote (radar) platforms
- Goals:
  1. Derive vertical profiles of cloud water content from radar returns for weapons assessment (Z-WC relationship),
  2. Apply knowledge gained from land-based data to shipborne radars in remote areas of the world, and
  3. Improve scientific understanding of cloud systems in both microphysical and dynamical senses to improve inputs in models.

Motivation for This Research

- Satisfy Goal 1 of CAPE2015 Field Experiment.
  - Obtain a radar reflectivity factor (Z)-measured cloud water content (WC) relationship.
- I have been involved with this research since data collection.

Aircraft Instrumentation

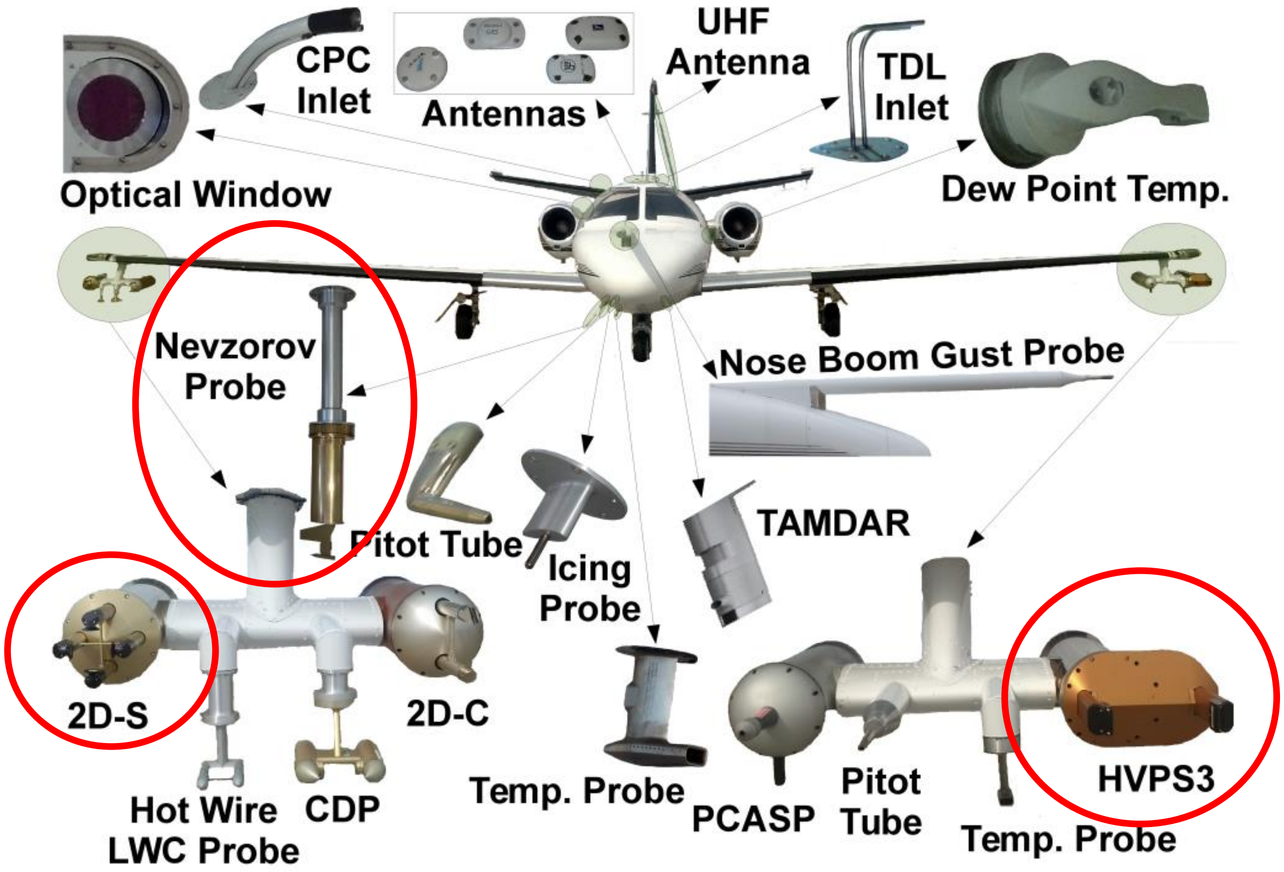

Two-Dimensional Stereographic Probe (2D-S)

- Optical array probe with two lasers oriented perpendicular (Lawson et al. 2006)
  - 128 10-um photodiodes
    - 10-2000 μm
  - Cloud particles shadow diodes and image is recorded
  - Data post-processing reconstructs images and sorts by diameter (29 size bins)
  - Anti-shatter tips

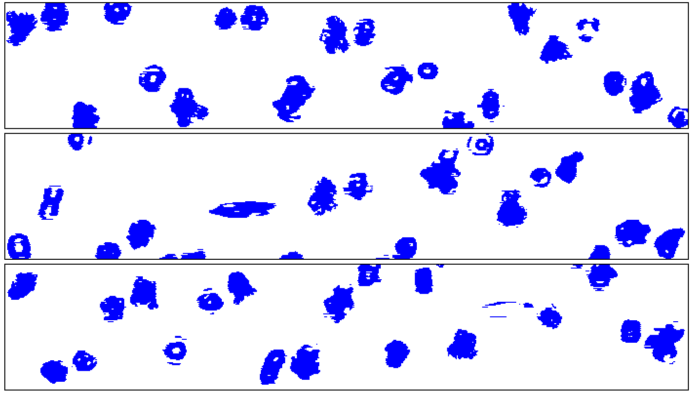

High-Volume Precipitation Spectrometer Version 3 (HVPS3)

- Optical array probe with one laser oriented horizontally (Lawson et al. 1993)
  - 128 150-um photodiodes
    - 150 µm to 3 cm
  - Cloud particles shadow diodes and image is recorded
  - Data post-processing reconstructs images and sorts by diameter (28 size bins)
  - Anti-shatter tips

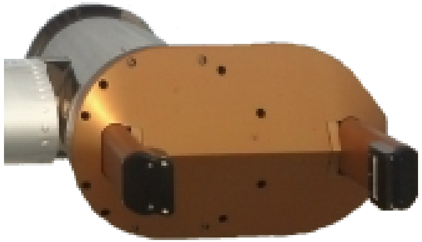

Nevzorov Water Content Probe

- Constant-temperature, hot-wire probe (Korolev et al. 1998)
  - Measures total (TWC) and liquid water content (LWC) with cone and wire, respectively
    - 0.003-3.0 g/m^3
  - Ice particles <4 mm melt entirely in TWC sensor (Korolev et al. 2013)
    - Larger particles may bounce out
  - Flight correct and base-line adjust data

Mid-Course Radar (MCR)

- Primary features:
  - C-band dual-polarization Doppler radar
  - 3 MW peak power & 0.2° beamwidth
  - Real-time satellite & aircraft tracking
  - Two waveforms:
    - **Narrowband** (37 m range resolution with two 75 km range windows
    - **Wideband** (0.5 m range resolution with two 400 m range windows
  - Range windows

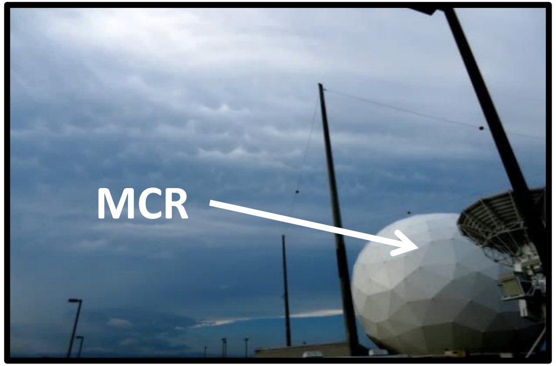

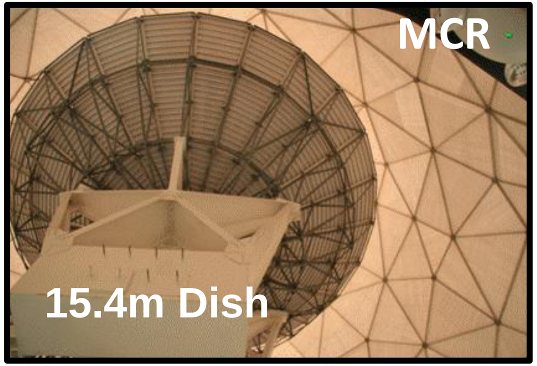

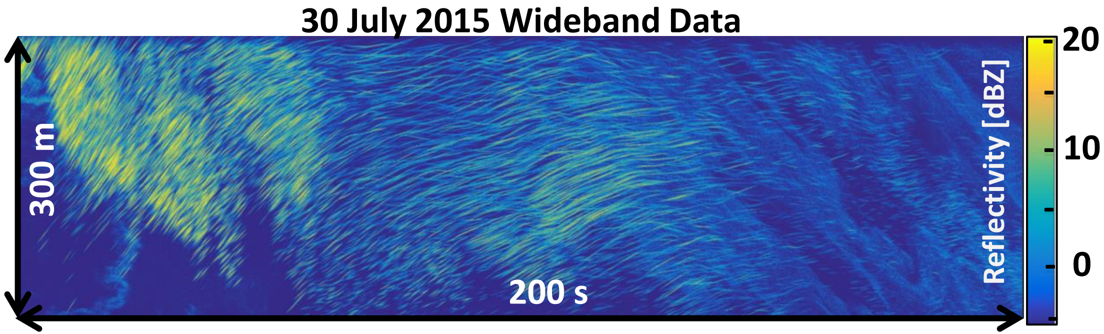

Schmidt et al. (2019); images courtesy of Jerome Schmidt

MCR

	MCR	UND WSR-74C	NWS WSR-88D
Antenna Diameter (m)	15.24	3.66	8.53
Beamwidth (degrees)	0.22	0.99	1.0
Peak Power (MW)	3.0	0.25	0.7
Frequency (GHz)	5.405-5.895	5.6	2.7-3.0
Pulse Repetition Frequency (Hz)	160 (both) or 320	250-1200	318-1304, 318-452
Pulse Length (μs)	12.5	0.6 or 2.0	1.57 or 4.5
Transmitter Polarization	Right circular	Linear, horizontal and vertical	Linear, horizontal and vertical
Receiver Polarization	Right and left circular	Linear, horizontal and vertical	Linear, horizontal and vertical
Maximum Range Resolution (m)	37	300	250
Minimum Range Resolution (m)	0.546	90	250
Sensitivity at 50 km Range (dBZ)	-36 (narrowband) -18 (wideband)	-8.0	-17.4

Schmidt et al. (2019); Rinehart (2010)

Scanning Strategies: Vertical Stare

Narrowband

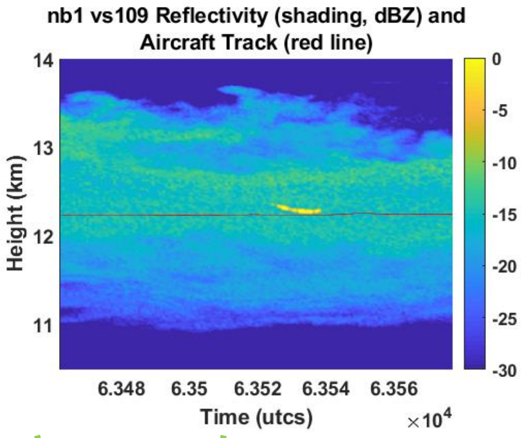

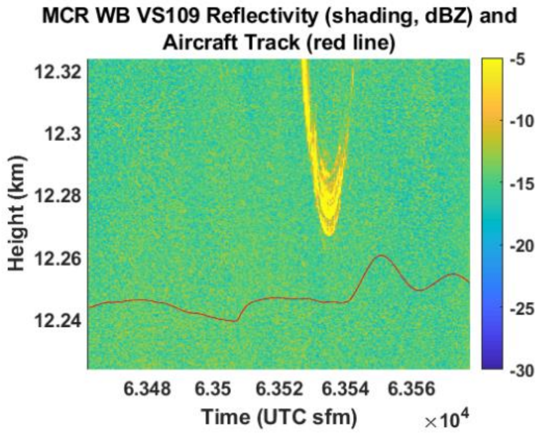

Wideband

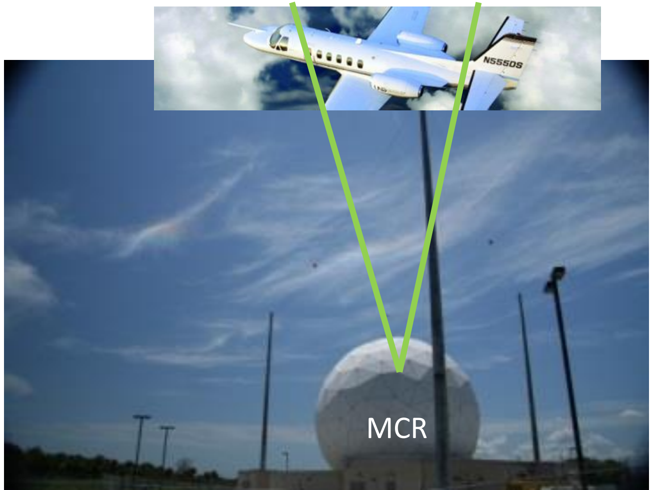

- Two co-location options:
  - MCR operates in vertical stare and waits for aircraft to cross into beam

Scanning Strategies: Aircraft Tracking

Narrowband

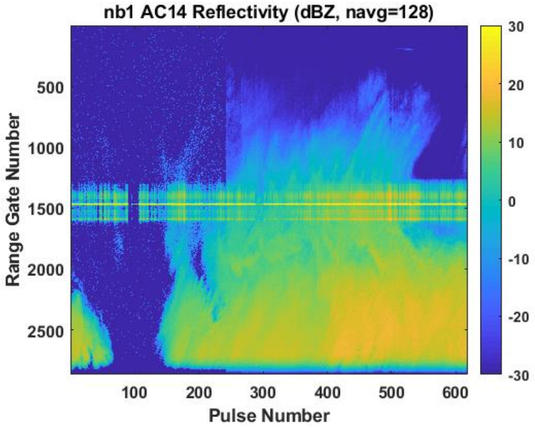

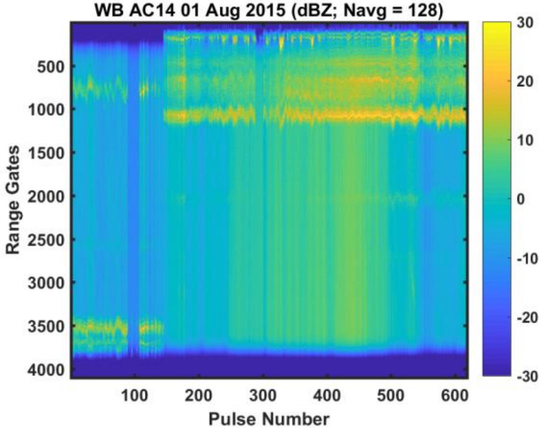

Wideband

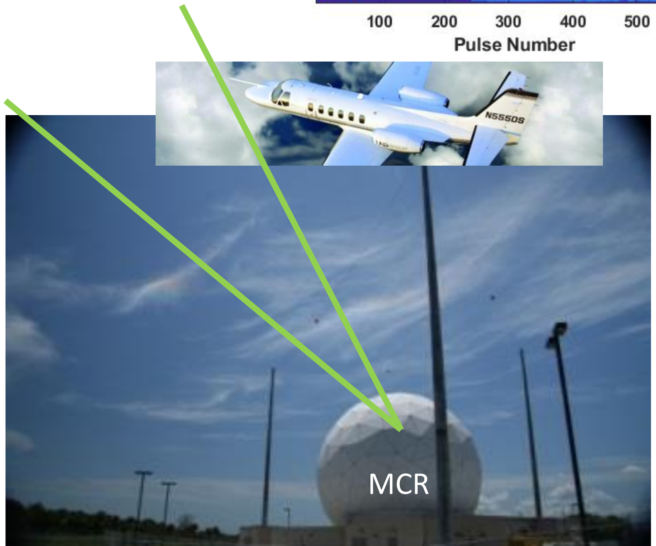

- Two co-location options:
  - Track aircraft through the sky by using downlinked GPS information and narrowband beam to lock onto aircraft and follow it with wideband set just ahead of aircraft for concurrent measurements.
- Use microphysical measurements to get WC and derive Z_e, compare Z_e to MCR Z to check agreement, and derive Z-WC relationship for vertical profiles.
- Will only discuss aircraft tracking results.

MCR

- Narrowband (NB) data contaminated from high returns from aircraft
  - Only wideband (WB) will be used in analysis in this study

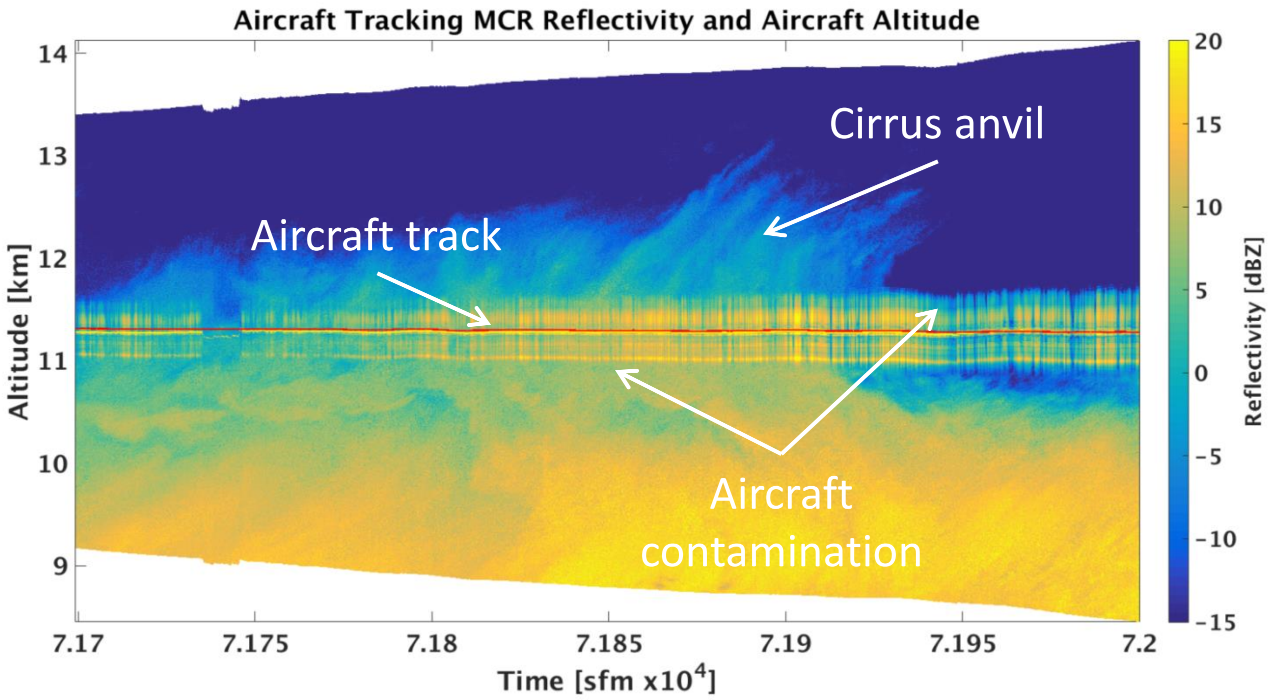

Aircraft and Radar Data Comparisons

- Derivation of in-situ equivalent radar reflectivity factor (Z_e)
  - Merge particle size distributions (PSDs) >100 µm from 2D-S and HVPS3 at 1,000 µm
    - 2D-S particle reconstruction effects are minimized by HVPS3 data
  - Total particle volume V_T per time step from merged PSD bin diameter D_i and particle concentration per size bin N_i

$$V_T = \sum_i \frac{\pi}{6} N_i {D_i}^3 \tag{1}$$

  - Effective particle density ρ_e from Nevzorov particle mass m_{Nev}

$$\rho_e = m_{Nev}/V_T \tag{2}$$

Aircraft and Radar Data Comparisons

- Derivation of in-situ equivalent radar reflectivity factor (Z_e)
  - Effective liquid particle size (d) per volume of merged PSD size bin V_n and density of water ρ_w

$$d = \sum_i \sqrt[3]{\frac{6}{\pi}\frac{V_i \rho_e}{\rho_w}} \tag{3}$$

    - Assumes mass of ice equals mass of water
  - Average *d* by number of bins that have concentration > 0 #/m^3 ($\bar{d}$)

$$Z = 10 \log \sum_i N_i {\bar{d}_i}^6 \tag{4}$$

$$Z_e = Z - 6.5\, dBZ \tag{5}$$

    - Dielectric factor of ice $|K|_i^2 = 0.208$ (Smith, 1984)

Uncertainty Analysis

- Uncertainty in Z_e only considers the error in concentration (Poisson Counting Statistics):

$$\epsilon_{rel} = n^{-1/2}, \tag{4}$$

  where *n* is the number of counts in a given size bin (Horvath 1990).

- Uncertainty in derived radar reflectivity is given by:

$$\delta z = \frac{\partial z}{\partial N} \delta N, \tag{5}$$

  where $z = Nd^6$ [*N* is particle concentration and *d* is liquid-equivalent diameter (Equation 3); *z* in $mm^6\ m^{-3}$] and δN is absolute uncertainty in particle concentration

- Normalize uncertainty per bin and sum (total relative uncertainty):

$$\epsilon_z = \sum_i \frac{\delta z_i}{z_i}. \tag{6}$$

Uncertainty Analysis

- 1 second vs. 10 second average
  - 1 second average captures natural variability within atmosphere
  - 10 second average lowers Z_e counting uncertainty
    - Capture systematic differences between data sets

Results

Data Analysis

- Analysis includes data using following criteria:
  - Temperatures <= -30 °C (assume all ice particles),
  - Nevzorov TWC > 0.005 g/m^3 (all measurements in-cloud), and
  - 2.5° <= pitch of aircraft <= 4.5° (assume level flight segments).

Date	Start (sfm)	End (sfm)	Min/Max Altitude (m)	Min/Max Temperature (°C)	Points/Percent (# / %)
2015/07/30	65,035	65,168	9,680 / 9,703	-30.8 / -30.0	133 / 100.0
2015/07/31	68,466	74,812	9,526 / 10,019	-34.2 / -30.1	1,760 / 27.7
2015/08/01	68,624	76,554	7,726 / 10,019	-47.2 / -30.2	2,036 / 25.7
2015/08/02	71,606	73,370	9,988 / 10,337	-36.7 / -32.7	467 / 26.5

- Particle size distributions (PSDs)
  - Each PSD is average of 1 min particle concentration data
  - 7.7-10.3 km, -30 to -47 °C
  - High concentrations of small particles except on 02 August
  - Large variability
    - Standard deviations

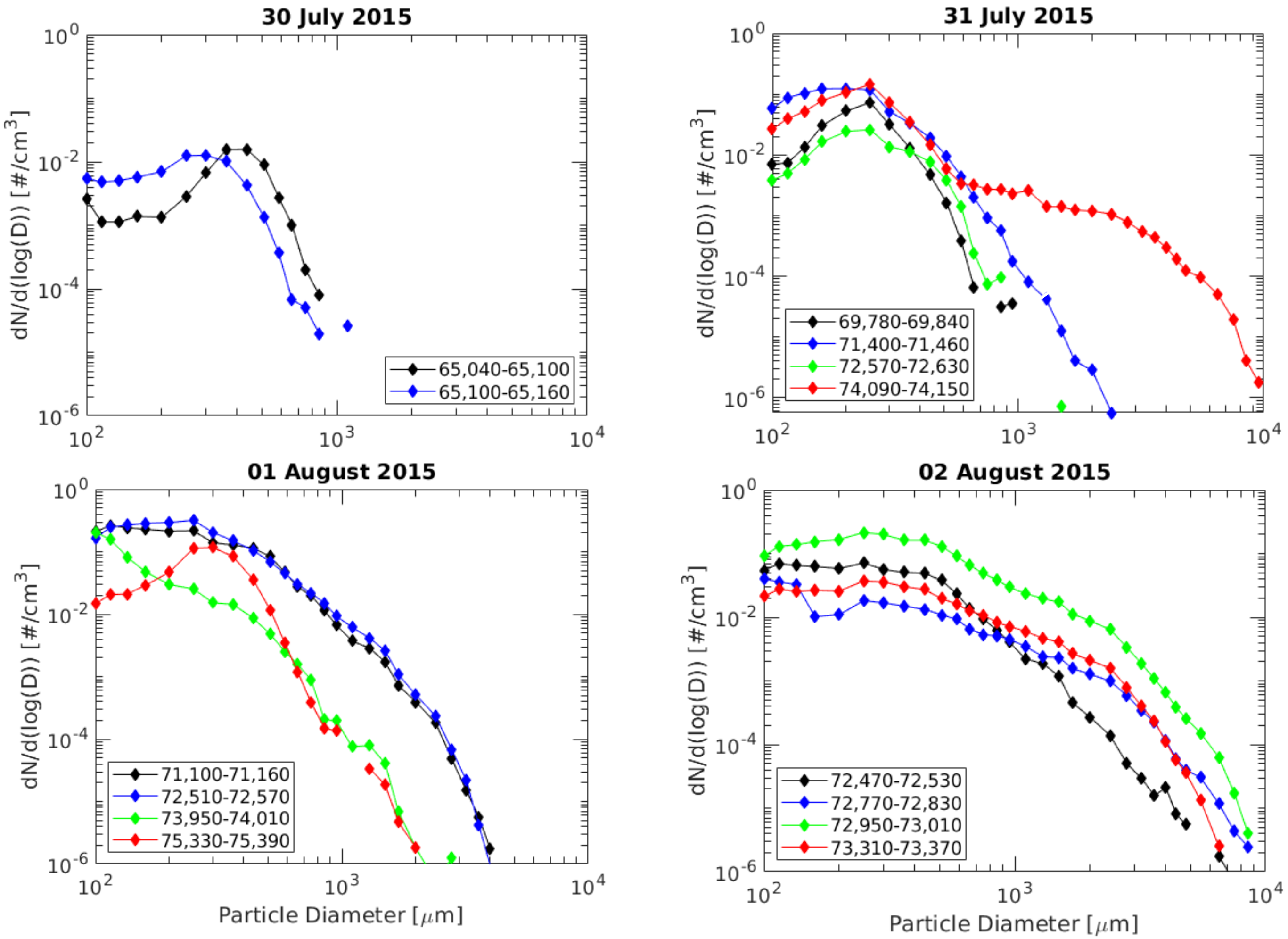

CAPE2015 Effective Particle Density

- Each dot is calculated using Equation 2.
- Red lines are: Heymsfield et al. (2004) (H2004), Cotton et al. (2013) (C2013), and Brown and Francis (1995)
- Exponential slope of power law line of best fit mostly agrees with previous studies.
  - Densities are smaller >300 µm

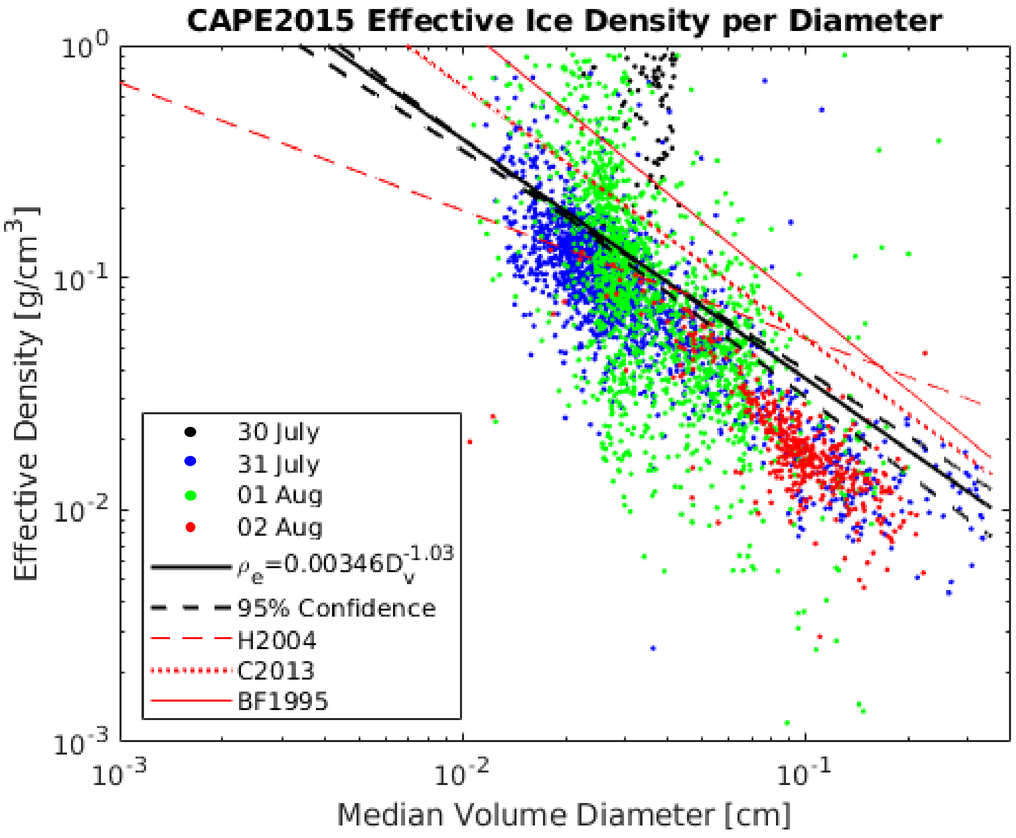

01 August 2015 Case Study

- 34 minutes of data where MCR tracks aircraft
  - AC13-AC16
- Analysis is completed using Data Analysis criteria

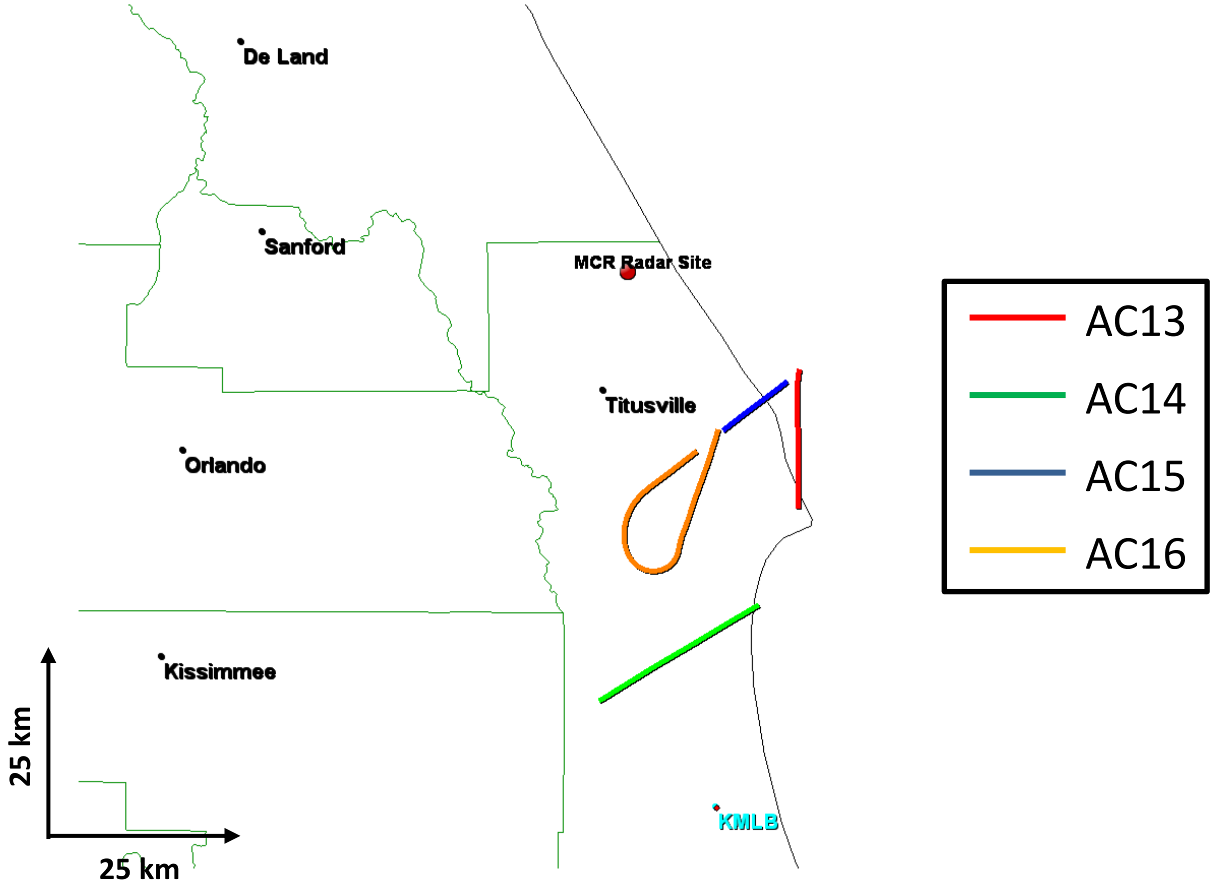

01 August 2015 Case Study

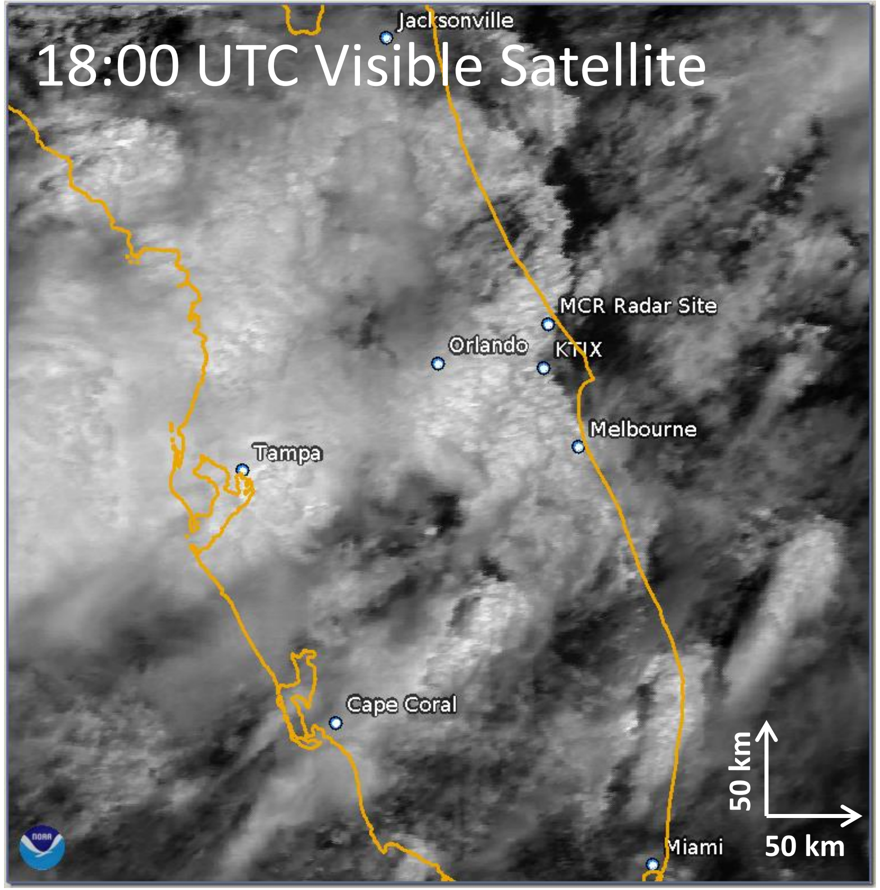

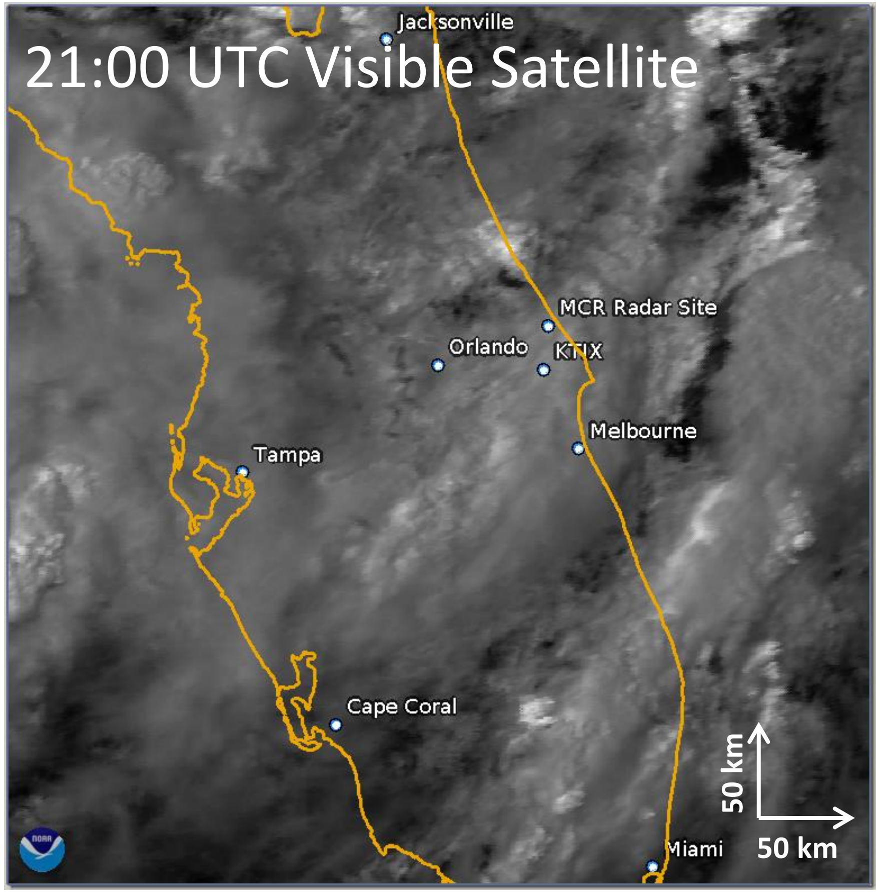

- Base reflectivity scan from KMLB nearest each case
- Stayed away from areas strong convection

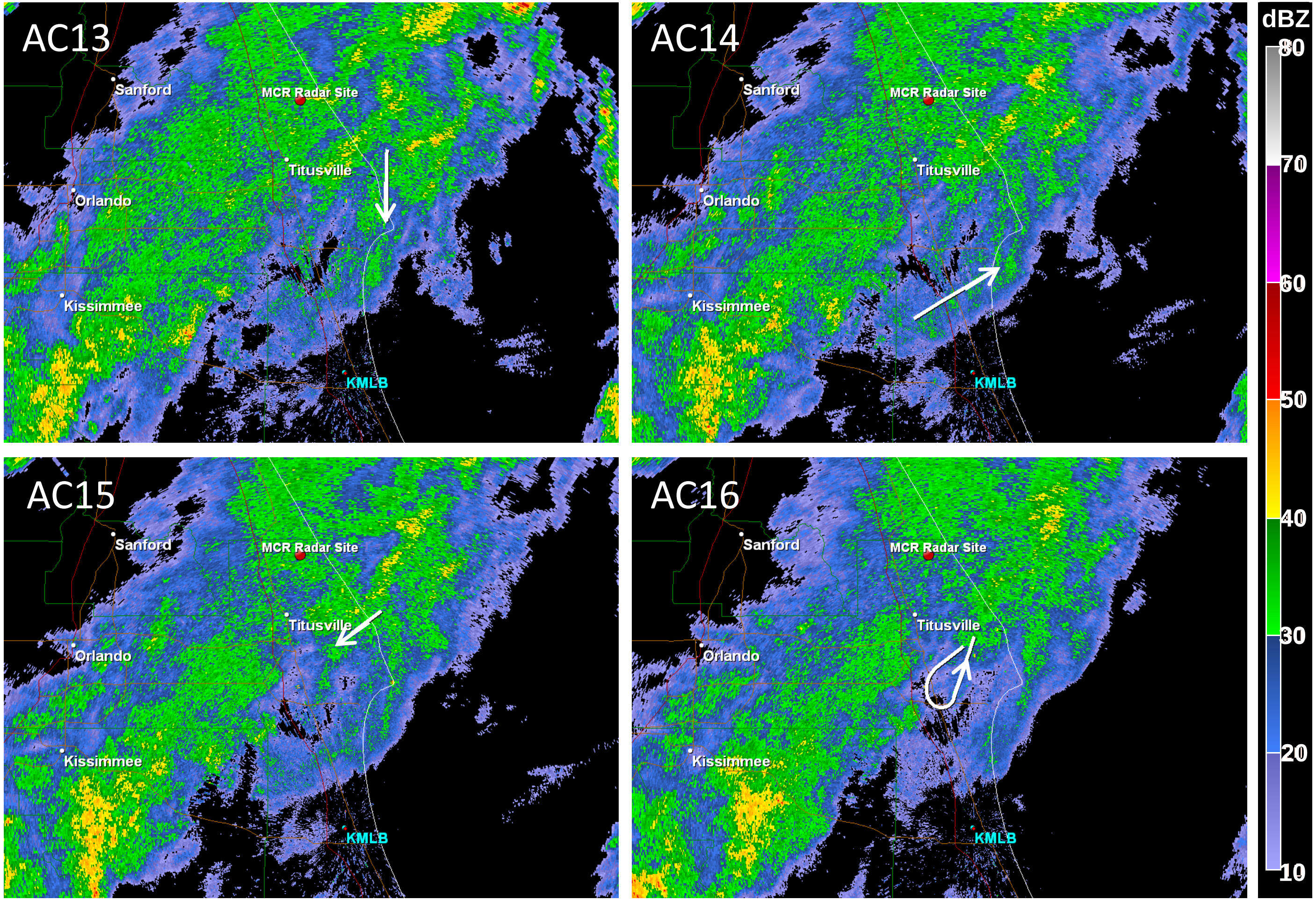

- Cross-sections of scans from KMLB for each case
- Note lack of data at flight levels

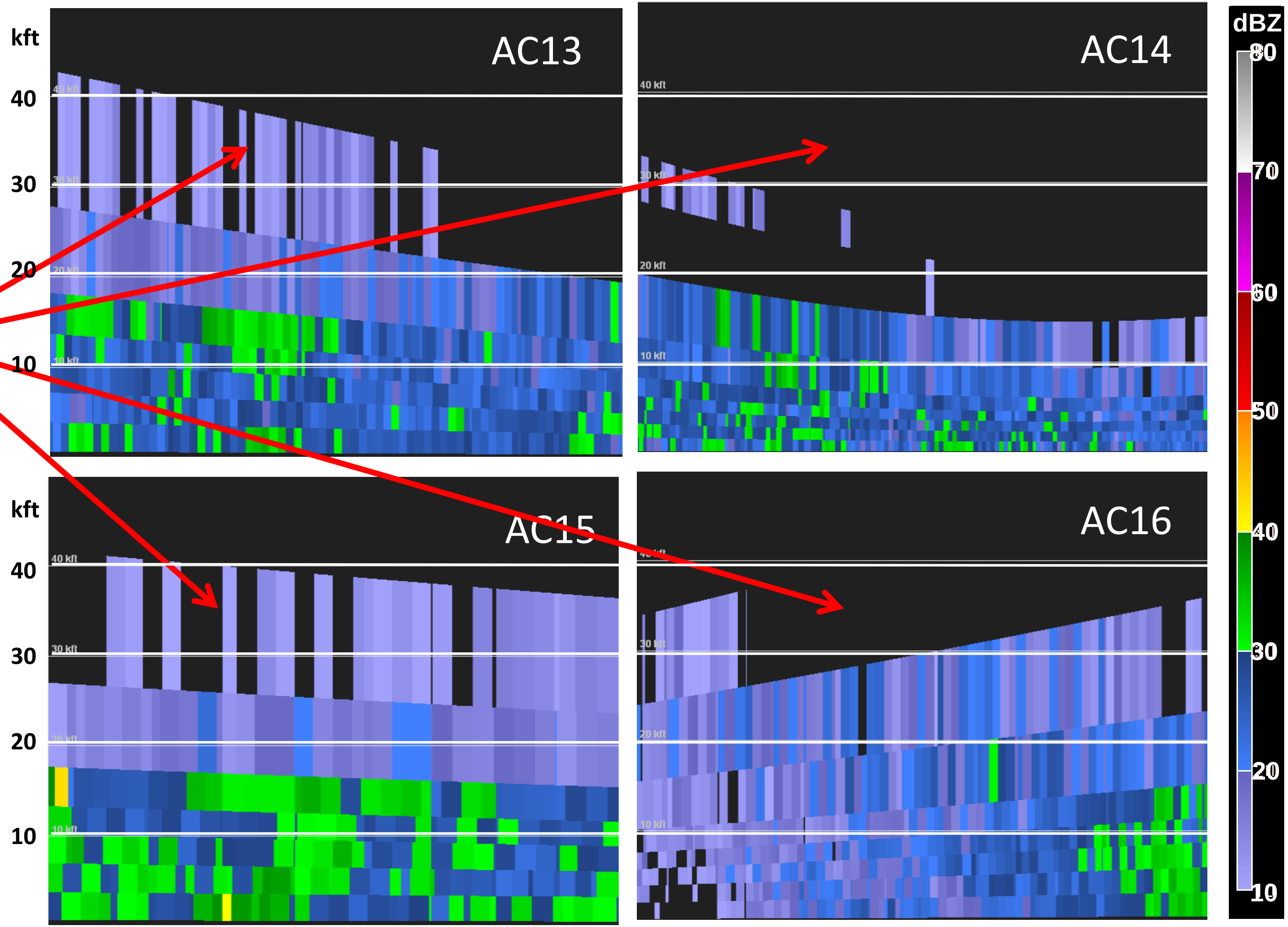

- Comparisons between Z_e and MCR reflectivity factor
  - 1 s average
  - Uncertainties up to ±455 % for Z_e
  - ±3 dBZ bias assumed for MCR

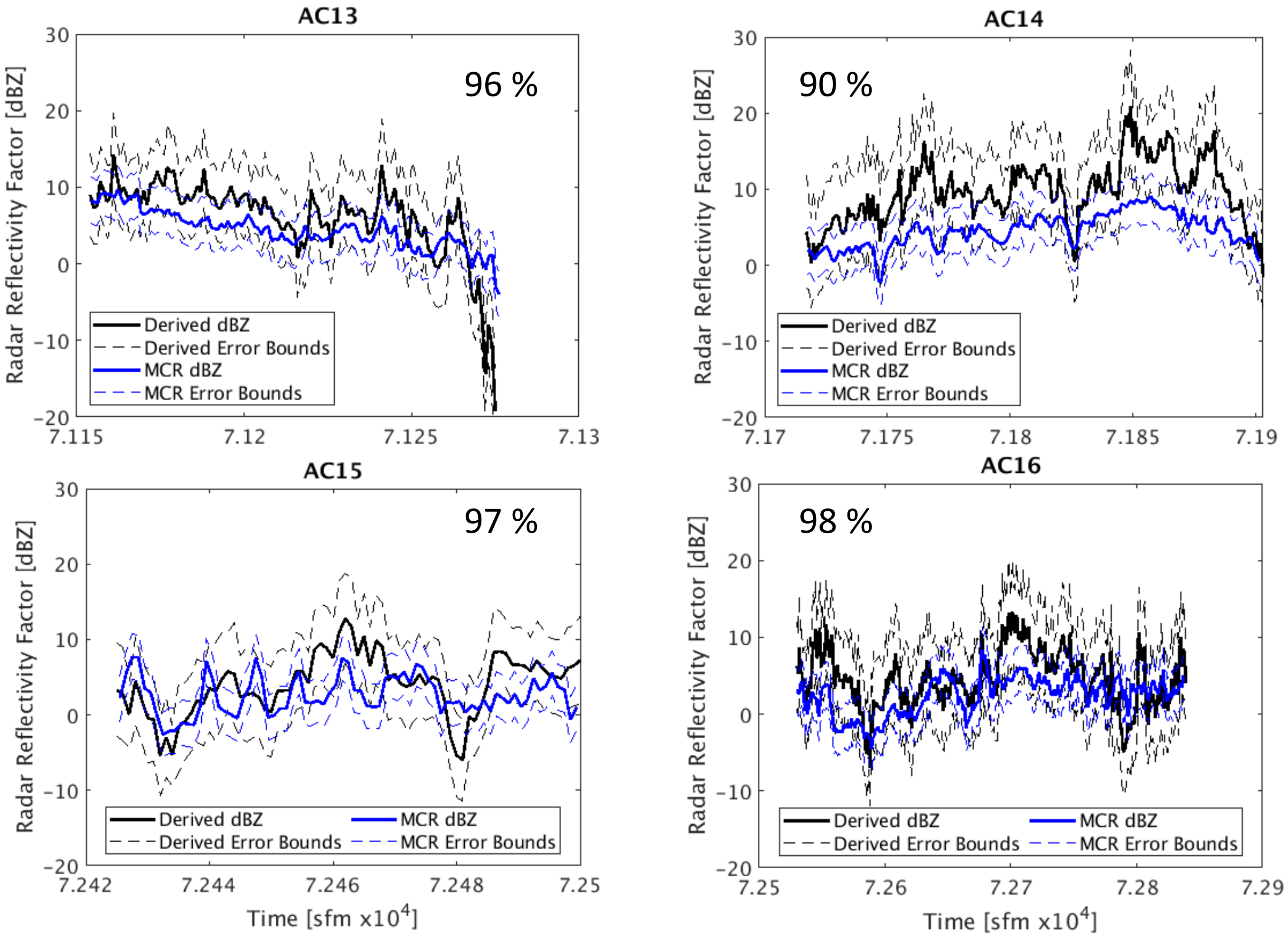

- Comparisons between Z_e and MCR reflectivity factor
  - 10 s average
  - Uncertainties up to ±150 % for Z_e
  - ±3 dBZ bias assumed for MCR

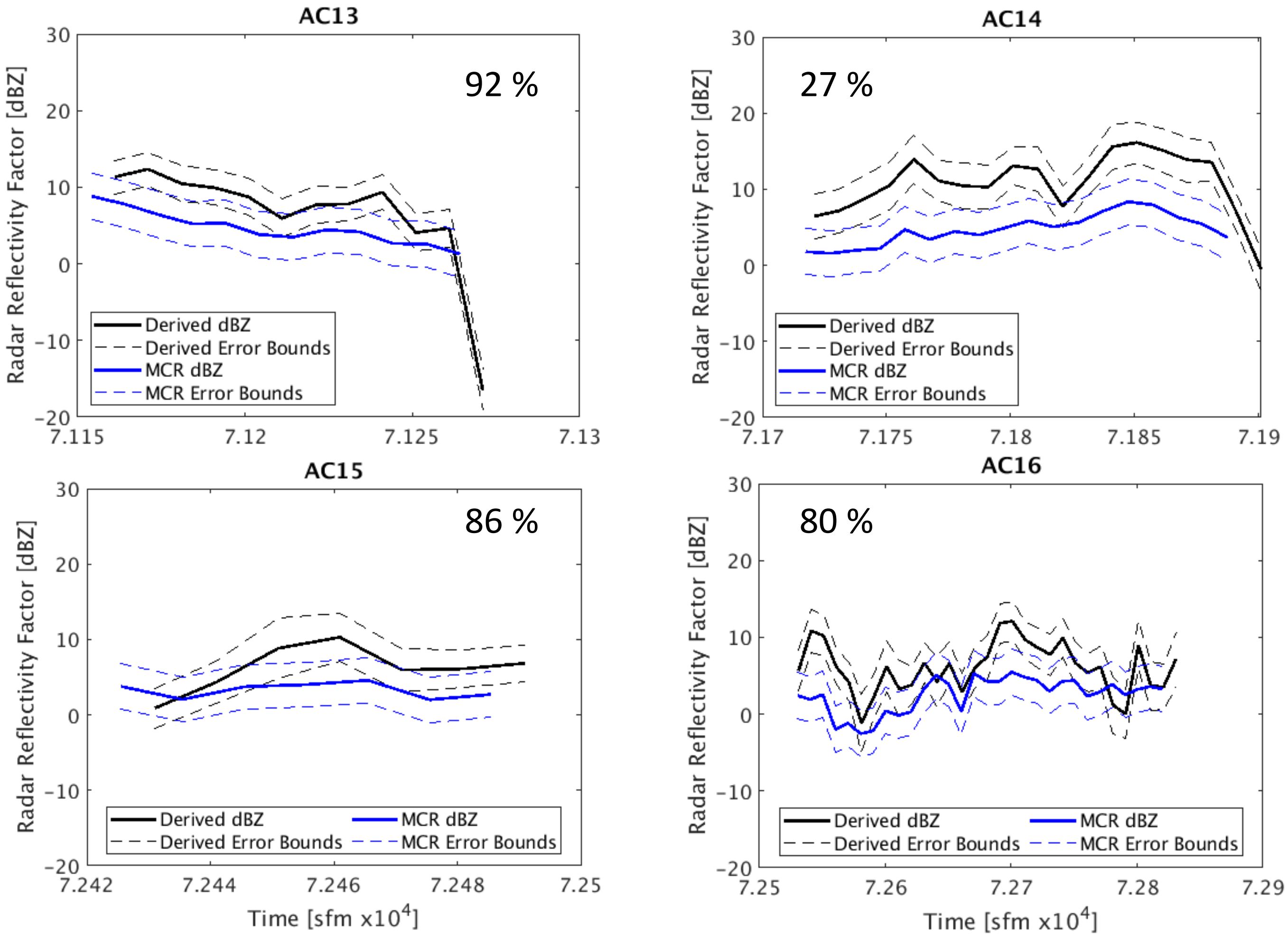

01 August 2015 Case Study

- Atmospheric conditions for all tracking data are very similar
  - AC14 case in not good agreement
    - 90 % and 27 %
  - AC13 case in good agreement
    - 96 % and 86 %

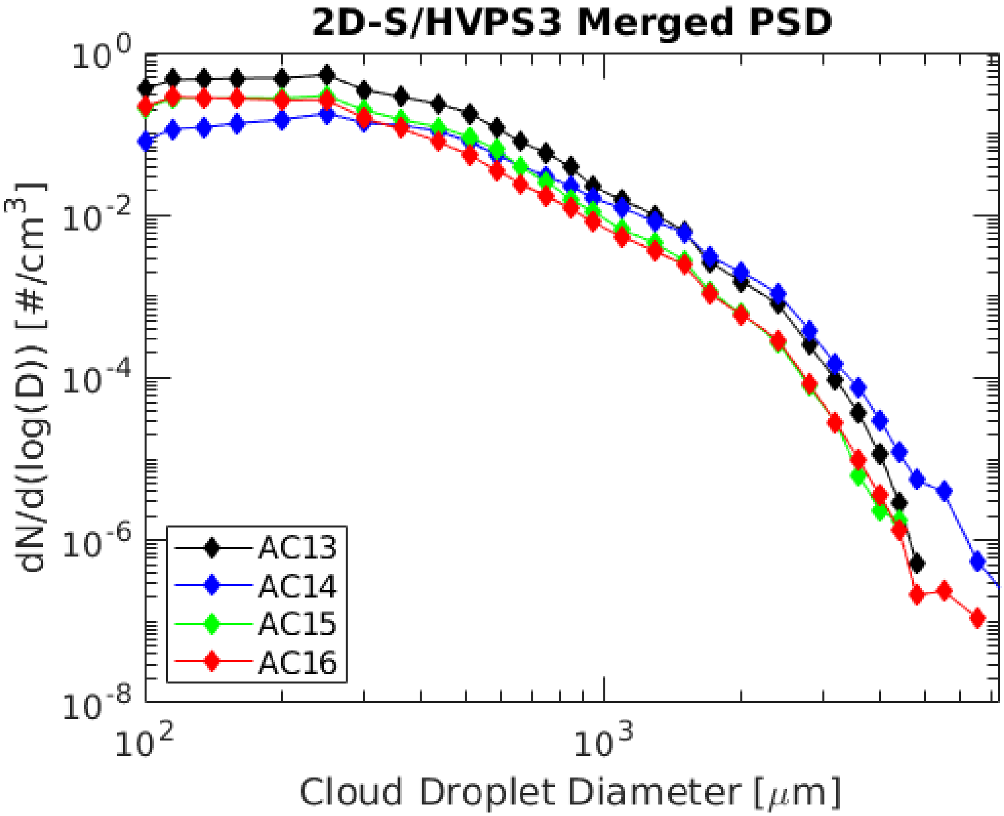

AC14

- Not good agreement
- ~11.3 km and -43.5 °C
- Particles greater than 500 µm observed
- Peak reflectivity factor at 12 dBZ and 2,500 µm

a)

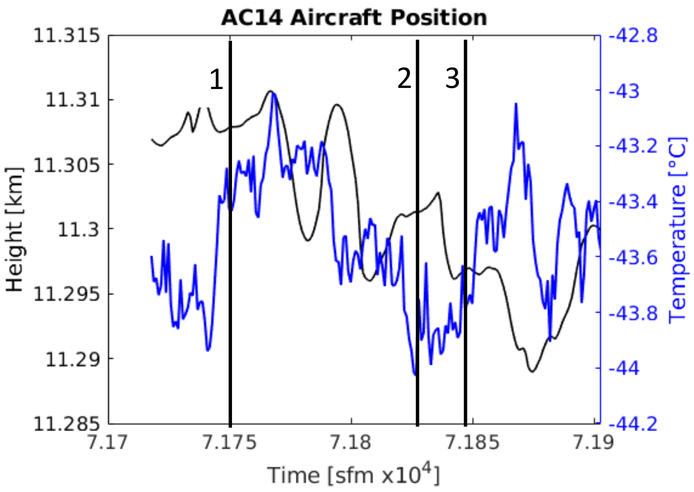

b)

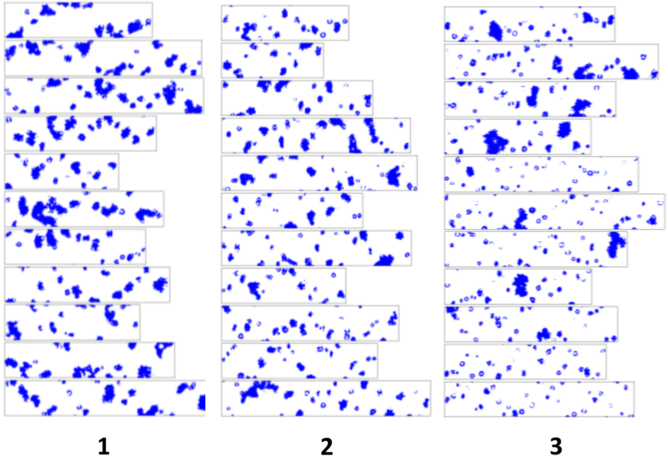

c)

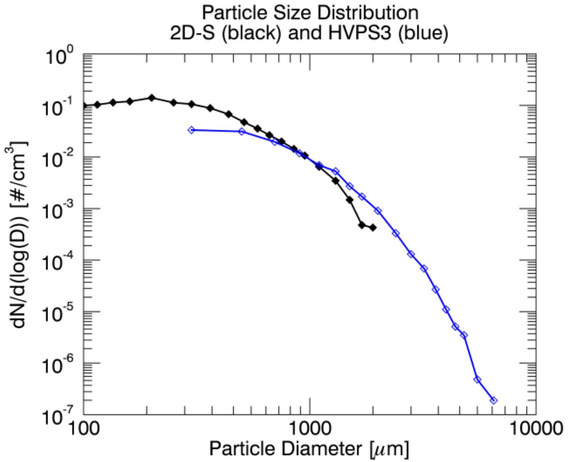

d)

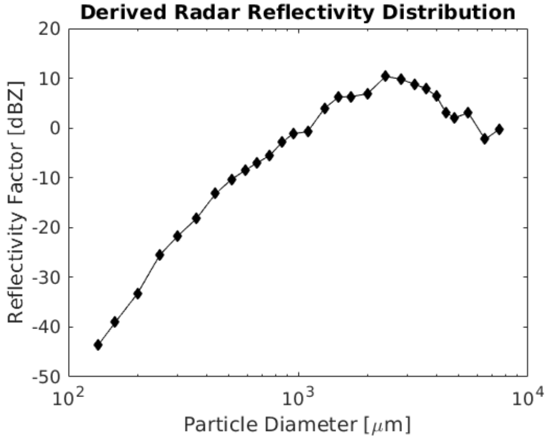

AC14

- Not good agreement
- 53 kg/m^3 average effective particle density
- Same order of magnitude for particle concentration and LED^6

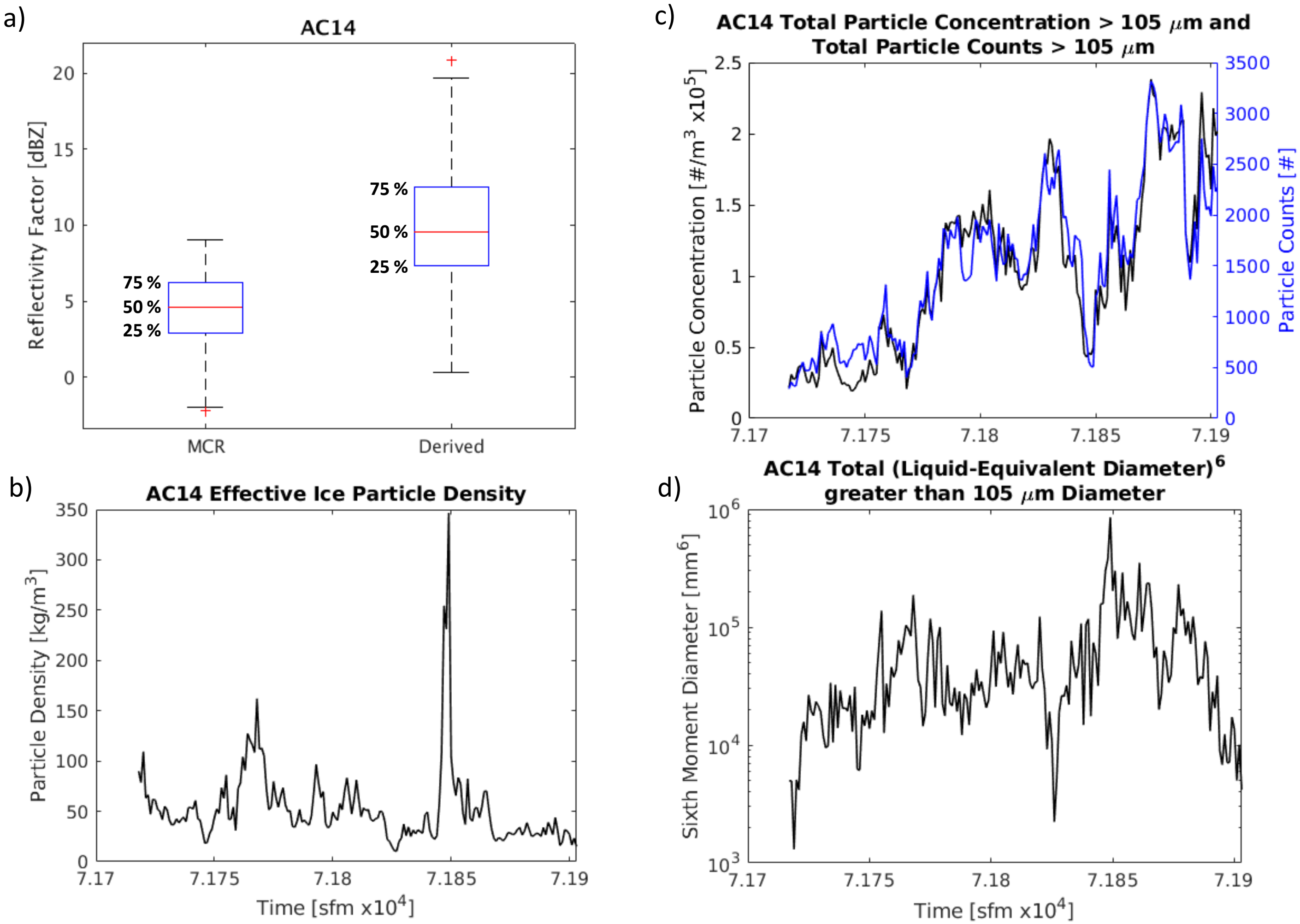

AC13

- Good agreement
- ~11.3 km and -43.4 °C
- Particles greater than 500 µm observed
- Peak reflectivity factor at 9 dBZ and 2,500 µm

a)

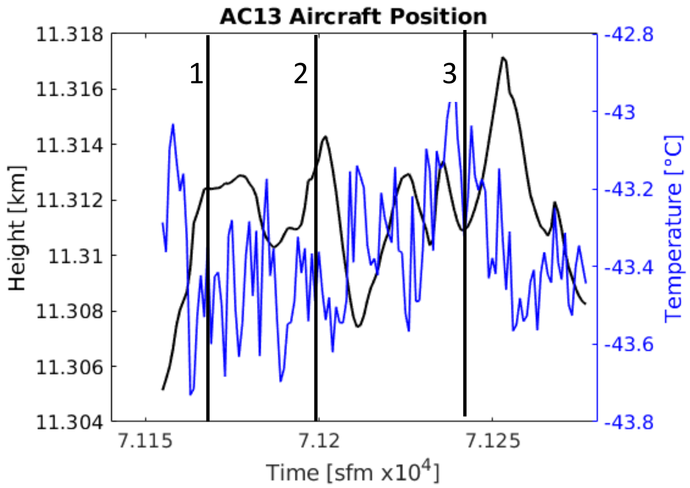

b)

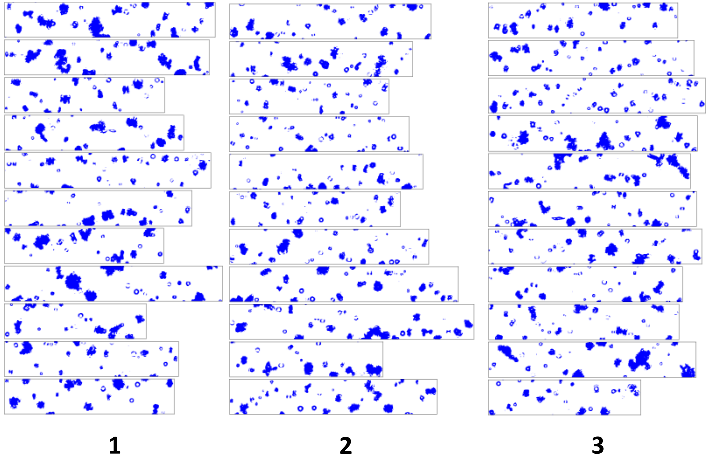

c)

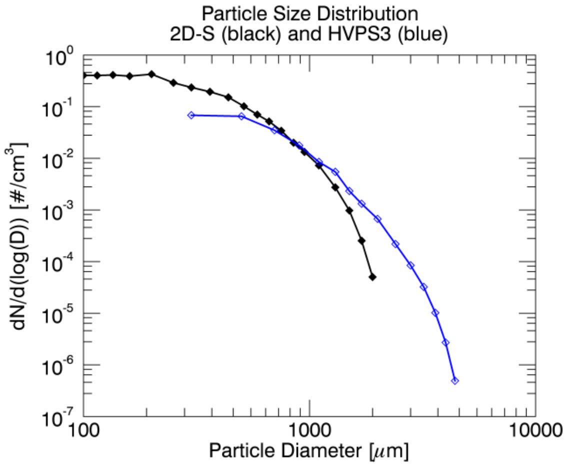

d)

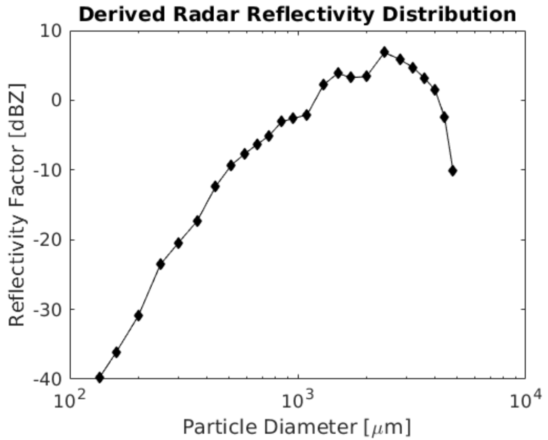

AC13

- Good agreement
- 37 kg/m^3 average effective particle density
- Same order of magnitude for particle concentration and LED^6

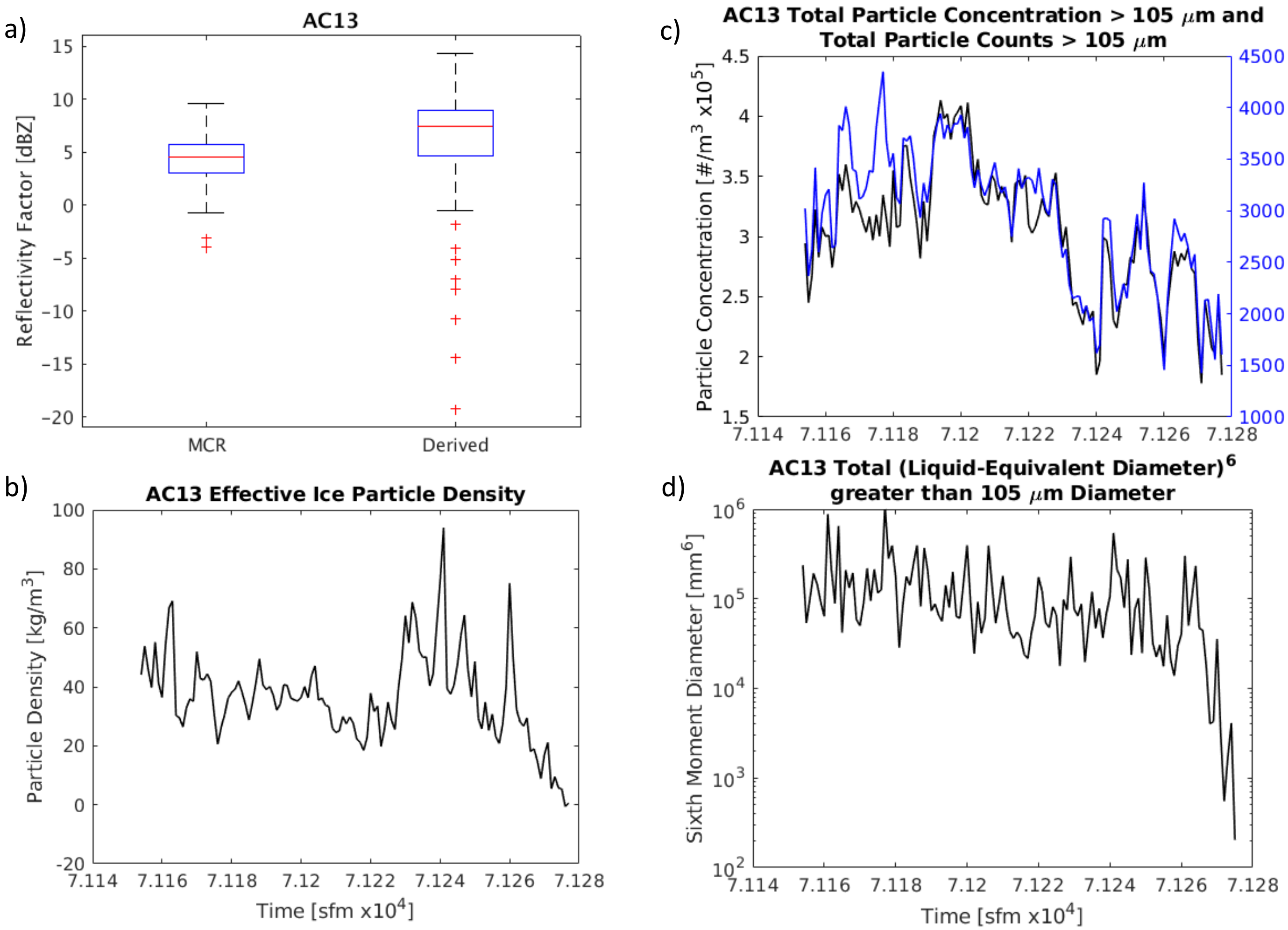

CAPE2015 MCR Reflectivity Factor-TWC

- Red lines are: Heymsfield et al. (2005) (H2005), Sassen (1987)* (S1987), and Heymsfield (1977)* (H1977)
  - Asterisks denote the use of reported mass-dimensional relationship
- Exponential slope of power law line of best fit mostly agrees with H2005.
  - CRYSTAL-FACE

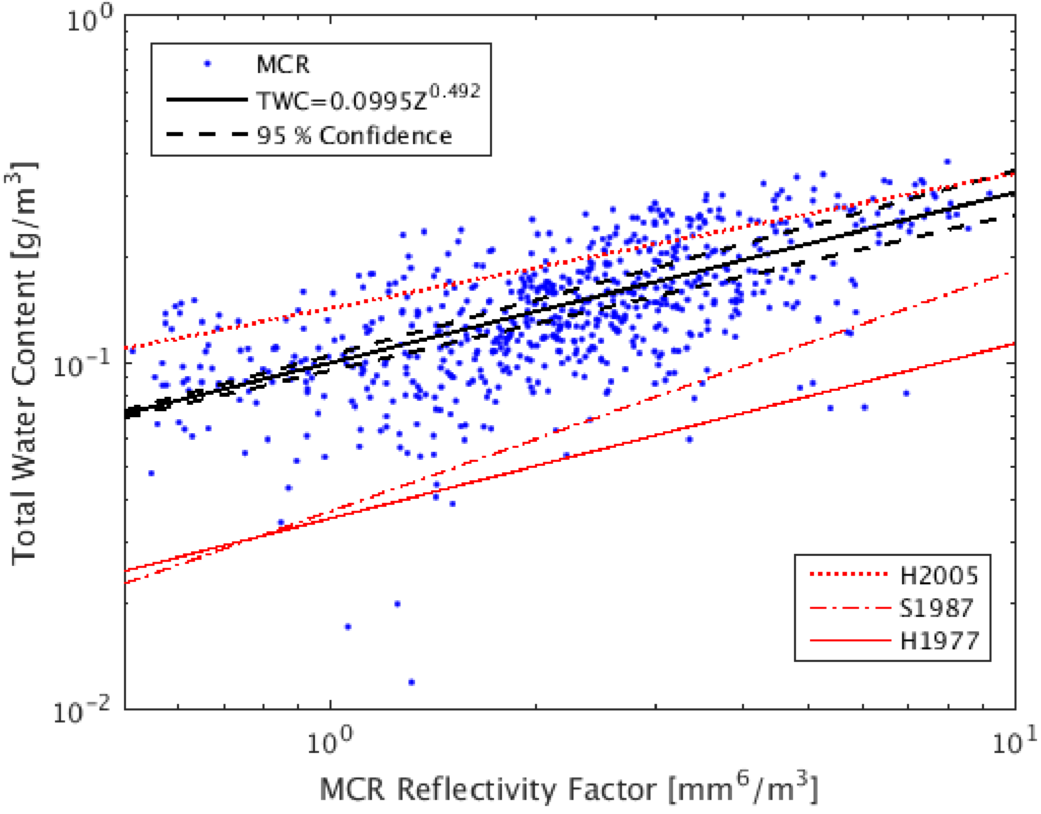

Conclusions

Conclusions

- The MCR successfully tracks aircraft and data can be co-located.
- The MCR and aircraft data agree with each other.
  - Except AC14
    - Broader HVPS3 PSD and higher effective densities than AC13 may be cause
  - Average of 95 % and 71 % of time at 1 and 10 s averaging, respectively
  - Z_e 1 s uncertainties up to ±455 %; 10 s uncertainties up to ±150 %
- Z_e is almost always higher than MCR reflectivity factor.
- Effective particle densities agree with published research.
- MCR Z-WC relationship agrees particularly well with CRYSTAL-FACE data.

Future Work

- Need more data for a more complete Z-WC vertical profile
  - This study covers 300 m and 13 dBZ
- Need to find true uncertainties in derived reflectivity factor
  - Optimizing equations and/or widths of bin sizes
- Analyze dual-polarization MCR data

Acknowledgements

- Funding from Naval Surface Warfare Center
  - Josh Hoover, NSWC Dahlgren Division
  - Mark Anderson, NSWC Dahlgren Division
- Special thanks
  - Peter Jones, L3 Interstate Electronics Corp., Anaheim, CA
  - The flight crew and everyone involved with CAPE2015
  - Committee
  - Mom, Dad, and family
  - Teachers and Professors
  - Friends

References

- Brown, P. R. A., and P. N. Francis, 1995: Improved Measurements of the Ice Water Content in Cirrus Using a Total-Water Probe. J. Atmos. Oceanic Technol., 12, 410–414, https://doi.org/10.1175/1520-0426(1995)012<0410:IMOTIW>2.0.CO;2.
- Cotton, R. J., and Coauthors, 2013: The effective density of small ice particles obtained from in situ aircraft observations of mid-latitude cirrus: Effective Density of Small Ice Particles. Quarterly Journal of the Royal Meteorological Society, 139, 1923–1934, https://doi.org/10.1002/qj.2058.
- Heymsfield, A. J., 1977: Precipitation Development in Stratiform Ice Clouds: A Microphysical and Dynamical Study. J. Atmos. Sci., 34, 367–381, https://doi.org/10.1175/1520-0469(1977)034<0367:PDISIC>2.0.CO;2.
- Heymsfield, A. J., A. Bansemer, C. Schmitt, C. Twohy, and M. R. Poellot, 2004: Effective ice particle densities derived from aircraft data. *Journal of the Atmospheric Sciences*, **61**, 982–1003, https://doi.org/10.1175/1520-0469(2004)061<0982:EIPDDF>2.0.CO;2.
- Heymsfield, A. J., Z. Wang, and S. Matrosov, 2005: Improved Radar Ice Water Content Retrieval Algorithms Using Coincident Microphysical and Radar Measurements. J. Appl. Meteor., 44, 1391–1412.
- Horvath, H., R. L. Gunter, and S. W. Wilkison, 1990: Determination of the Coarse Mode of the Atmospheric Aerosol Using Data from a Forward-Scattering Spectrometer Probe. Aerosol Science and Technology, 12, 964–980, https://doi.org/10.1080/02786829008959407.
- Jensen, E., D. Starr, and O. B. Toon, 2004: Mission investigates tropical cirrus clouds. *Eos, Transactions American Geophysical Union*, **85**, 45–50, https://doi.org/10.1029/2004EO050002.
- Korolev, A., J. W. Strapp, G. A. Isaac, and E. Emery, 2013b: Improved Airborne Hot-Wire Measurements of Ice Water Content in Clouds. J. Atmos. Oceanic Technol., 30, 2121–2131, https://doi.org/10.1175/JTECH-D-13-00007.1.
- Korolev, A. V., J. W. Strapp, G. A. Isaac, and A. N. Nevzorov, 1998: The Nevzorov Airborne Hot-Wire LWC–TWC Probe: Principle of Operation and Performance Characteristics. Journal of Atmospheric and Oceanic Technology, 15, 1495–1510, https://doi.org/10.1175/1520-0426(1998)015<1495:TNAHWL>2.0.CO;2.
- Lawson, R. P., R. E. Stewart, J. W. Strapp, and G. A. Isaac, 1993: Aircraft observations of the origin and growth of very large snowflakes. Geophys. Res. Lett., 20, 53–56.
- Lawson, R. P., D. O'Connor, P. Zmarzly, K. Weaver, B. Baker, Q. Mo, and H. Jonsson, 2006: The 2D-S (Stereo) Probe: Design and Preliminary Tests of a New Airborne, High-Speed, High-Resolution Particle Imaging Probe. Journal of Atmospheric and Oceanic Technology, 23, 1462–1477, https://doi.org/10.1175/JTECH1927.1.
- Schmidt, J. M. and Coauthors, 2019: Radar detection of individual cloud hydrometeors. *Bull. Amer. Meteor. Soc*, **In review**.
- Sassen, K., 1987: Ice Cloud Content from Radar Reflectivity. J. Climate Appl. Meteor., 26, 1050–1053, https://doi.org/10.1175/1520-0450(1987)026<1050:ICCFRR>2.0.CO;2.
- Smith, P., 1984: Equivalent radar reflectivity factors for snow and ice particles. J. Climate Appl. Meteor., 23, 1258–1260.

Extra Slides

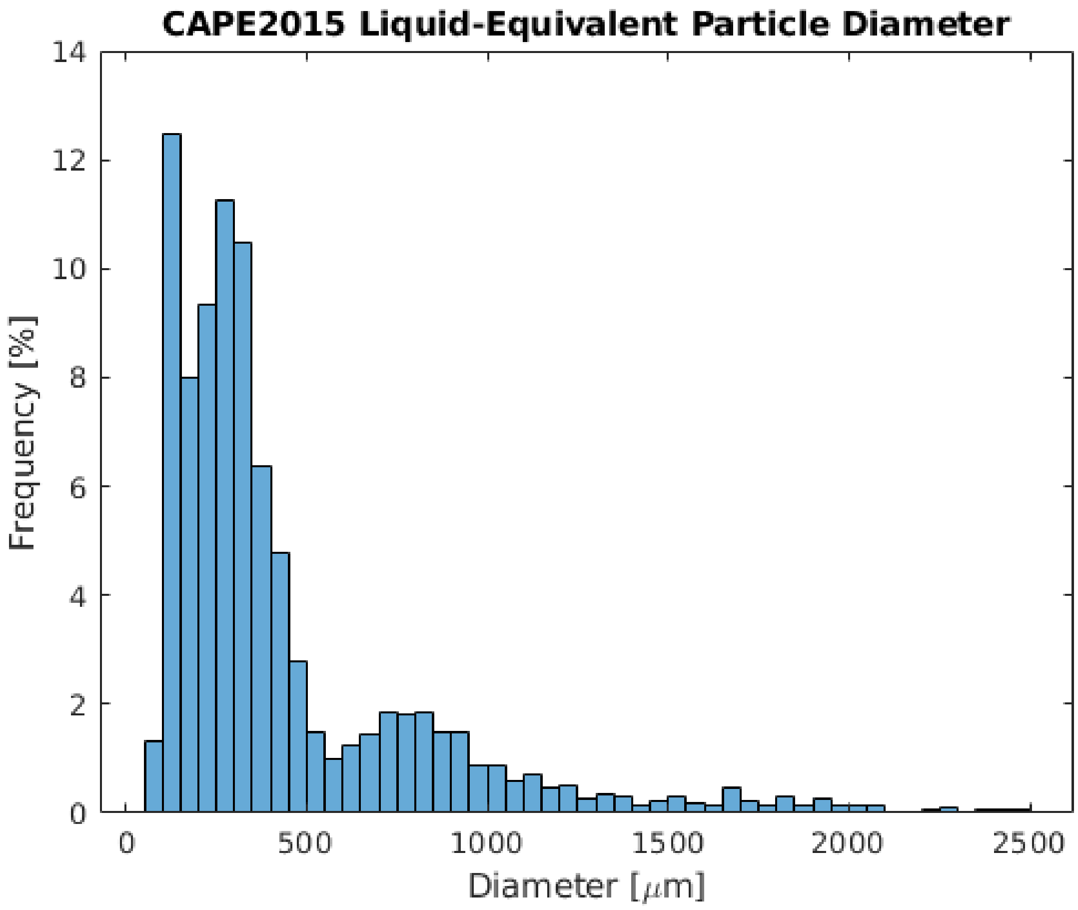

CAPE2015 Liquid-Equivalent Particle Diameter
Frequency [%]
Diameter [μm]
0
2
4
6
8
10
12
14
0
500
1000
1500
2000
2500

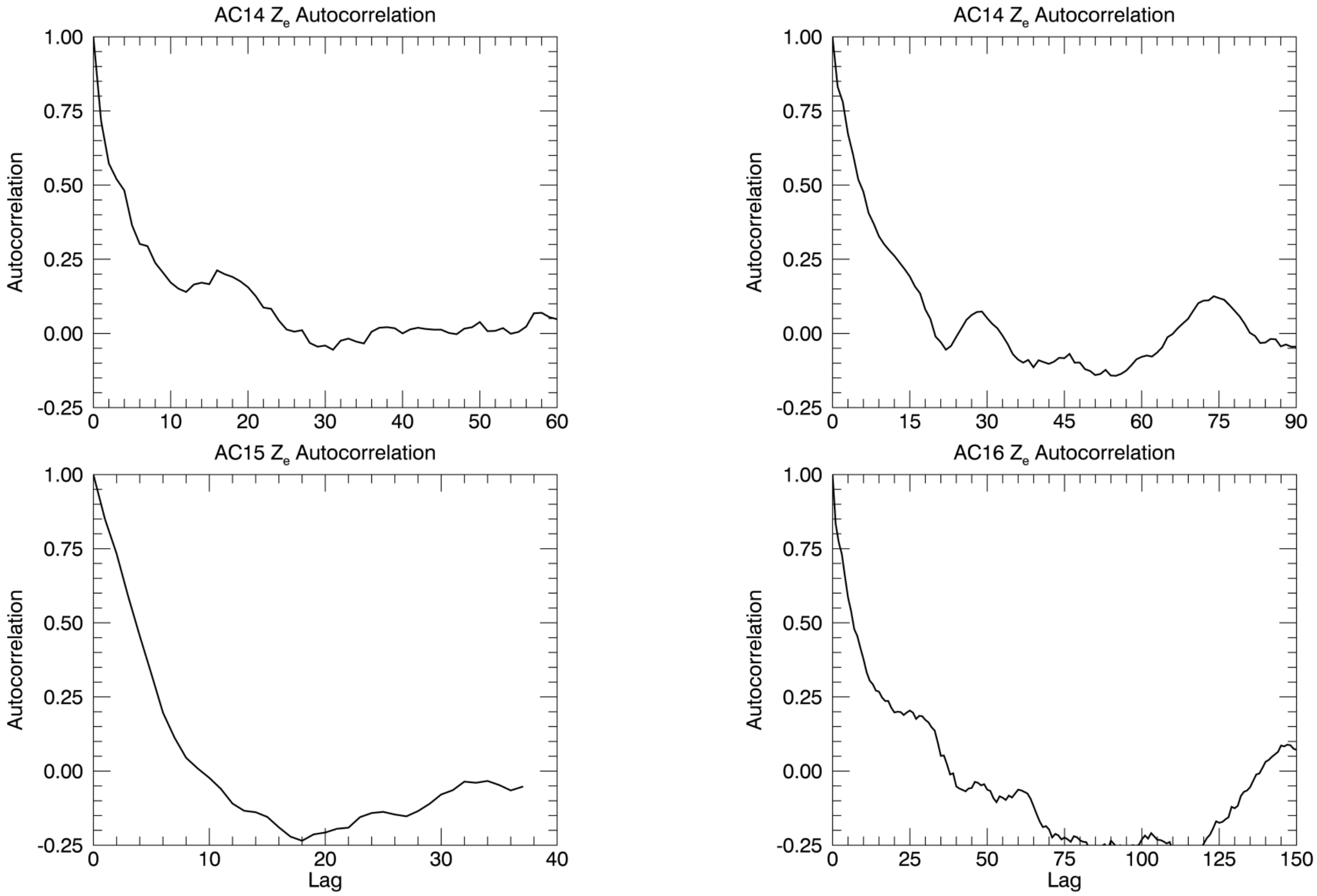

AC14 Z_e Autocorrelation
Autocorrelation
1.00
0.75
0.50
0.25
0.00
-0.25
0
10
20
30
40
50
60
AC14 Z_e Autocorrelation
Autocorrelation
0
15
30
45
60
75
90
AC15 Z_e Autocorrelation
Autocorrelation
0
10
20
30
40
Lag
AC16 Z_e Autocorrelation
Autocorrelation
0
25
50
75
100
125
150
Lag

Background: Z-IWC Relationship

- Heymsfield (1977)
  - Derived Z-IWC relationship using measured IWC to predict radar reflectivity factor of stratiform ice clouds at various altitudes, temperatures, and synoptic conditions.
  - After solving for IWC, equation becomes:

$$IWC = 10^{0.5051 \log Z - 1.452}.$$

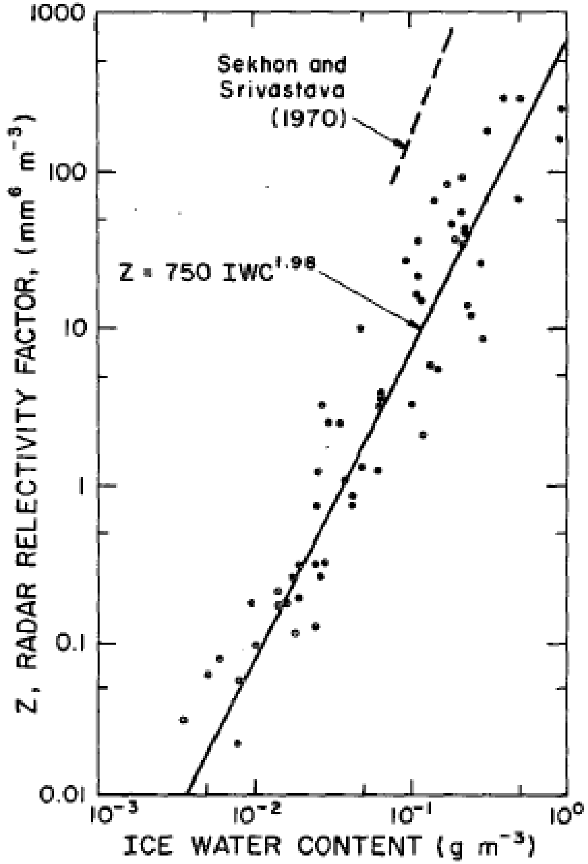

Background: Z-IWC Relationship

- Sassen (1987)
  - Derived ice-equivalent radar reflectivity factor $Z_i = 1.18Z_c$, where Z_c is liquid-equivalent radar reflectivity factor from Smith (1984) for ice mass content from upper portions of deep convection.
  - Line 2a is Z-IWC relationship from Sassen (1987) and Line 2b is relationship from Heymsfield (1977).

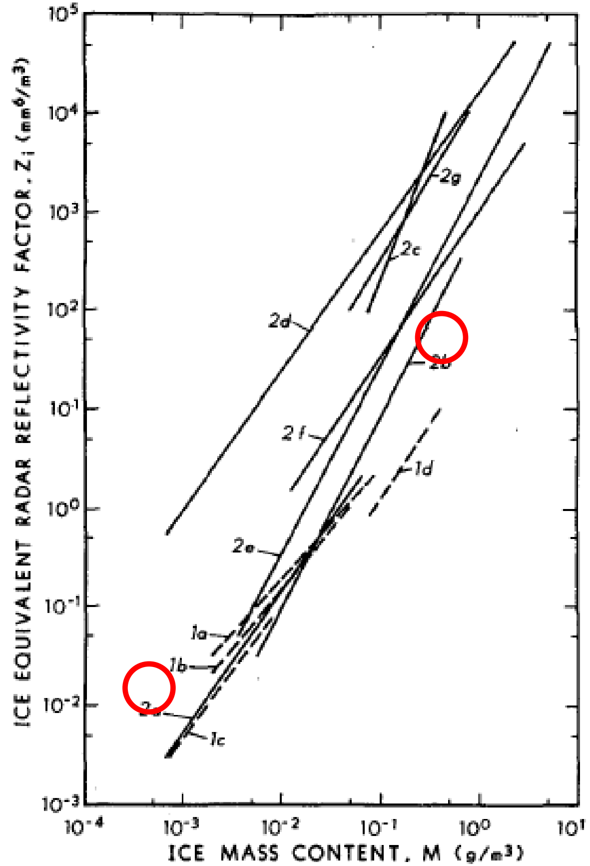

Background: Effective Ice Particle Density

- Heymsfield et al. (2004)
  - CRYSTAL-FACE (Jensen 2004)
  - Used similar instrumentation as in CAPE2015.
    - Citation Research Aircraft and HVPS mainly
  - Median mass diameter from a gamma-distributed particle size distribution vs. mean effective particle density.
  - Relationship is valid for convectively generated anvils.
  - Error sources include:
    - Using two-dimensional data to derive effective ice particle densities
    - Breakup of large particles in the inlet of probes
    - Under-sampling of large particles by cloud water content instrument

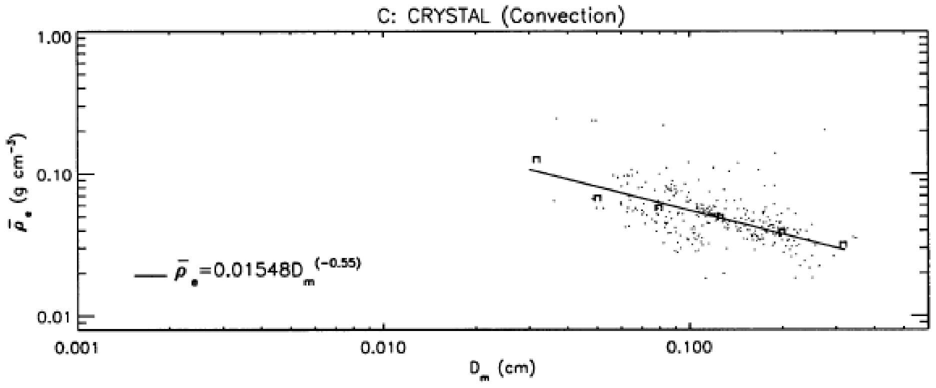

Background: Effective Ice Particle Density

- Cotton et al. (2013)
  - Derived mass-dimensional relationship for use in calculating effective ice particle densities using 2D-S and Nevzorov.
    - Drift in Nevzorov base-line measurements were corrected.
  - Concluded small ice particles (diameter <70 µm) have constant effective ice density of 700 kg/m³.